

Supporting Information

A CHEF-driven fluorescent turn-on probe for sensitive and rapid Al³⁺ detection in live MDA-MB-231 cells

Rahul Naskar,[†] Gita Rani Murmu,[†]Subrata Mandal,[†]Rimi Mukherjee,[‡]Arpan Halder,[†]Amitav Biswas,[†]Moumita Ghosh,[†]Saswati Gharami,^{†*}Nabendu Murmu^{‡‡*} and Tapan K. Mondal^{†*}

[†]Department of Chemistry, Jadavpur University, Kolkata- 700032, India. E-mail: tapank.mondal@jadavpuruniversity.in

[‡]Department of Signal Transduction and Biogenesis Amines (STBA), Chittaranjan National Cancer Institute, Kolkata- 700026, India.

^{‡‡}Dr. Giri Cancer Research Institute, India. E-mail: nabendu_m64@giridiag.in

CONTENTS

Fig. S1. ¹H-NMR spectrum of PIMB

Fig. S2. ¹³C-NMR spectra of PIMB

Fig. S3. ¹H-NMR spectrum of PIMB-Al³⁺

Fig. S4. IR spectra of PIMB

Fig. S5. IR spectra of PIMB-Al³⁺

Fig. S6. ESI mass spectra of PIMB

Fig. S7. ESI mass spectra of PIMB-Al³⁺

Fig. S8. Emission spectra of PIMB in different solvents.

Fig. S9. Emission spectra of PIMB-Al³⁺ in different solvents.

Fig. S10. Change in UV-Vis spectra of the probe (PIMB) (15 μM) upon addition of 2 equivalent of various metal ions (30 μM).

Fig. S11: Excitation spectra of PIMB and the PIMB-Al³⁺ complex.

Fig. S12. Change in emission spectra of the probe (PIMB) (15 μM) upon addition of 2 equivalent of various metal ions (30 μM)

Fig. S13. Job's plot of PIMB for Al³⁺

Fig. S14. Mole ratio plot of PIMB for Al³⁺

Fig. S15. Linear response curve of PIMB depending on Al³⁺ concentration

Fig. S16. Determination of association constant of PIMB for Al³⁺ from fluorescence titration data

Fig. S17. Stability study of PIMB and PIMB-Al³⁺

Fig. S18. pH study of PIMB for Al³⁺

Fig. S19. Change in emission spectra of PIMB (15 μM) upon gradual addition of Al³⁺ (0-30 μM) in MeOH/H₂O (1/1, v/v) where H₂O part is pond water.

Fig. S20. Change in emission spectra of PIMB (15 μM) upon gradual addition of Al³⁺ (0-30 μM) in MeOH/H₂O (1/1, v/v) where H₂O part is pond water.

Fig. S21. Optimized structure of PIMB calculated by DFT/B3LYP/6-31+G(d) method

Fig. S22. Optimized structure of PIMB-Al³⁺ calculated by DFT/B3LYP/6-31+G(d) method

Fig. S23. Contour plots of some selected molecular orbitals of PIMB

Fig. S24. Contour plots of some selected molecular orbitals of PIMB-Al³⁺

Determination of emission quantum yield (Φ) of PIMB and its complex with Al³⁺

Table S1: Table of mole fractions for Job's plot of PIMB and Al³⁺

Table S2. Energy and compositions of some selected molecular orbitals of PIMB-Al³⁺

Table S3. Vertical electronic transitions calculated by TDDFT/B3LYP/CPCM method for PIMB and PIMB-Al³⁺ in methanol

Table S4: The comparison of the present probe (PIMB) with some previous probes for Al³⁺

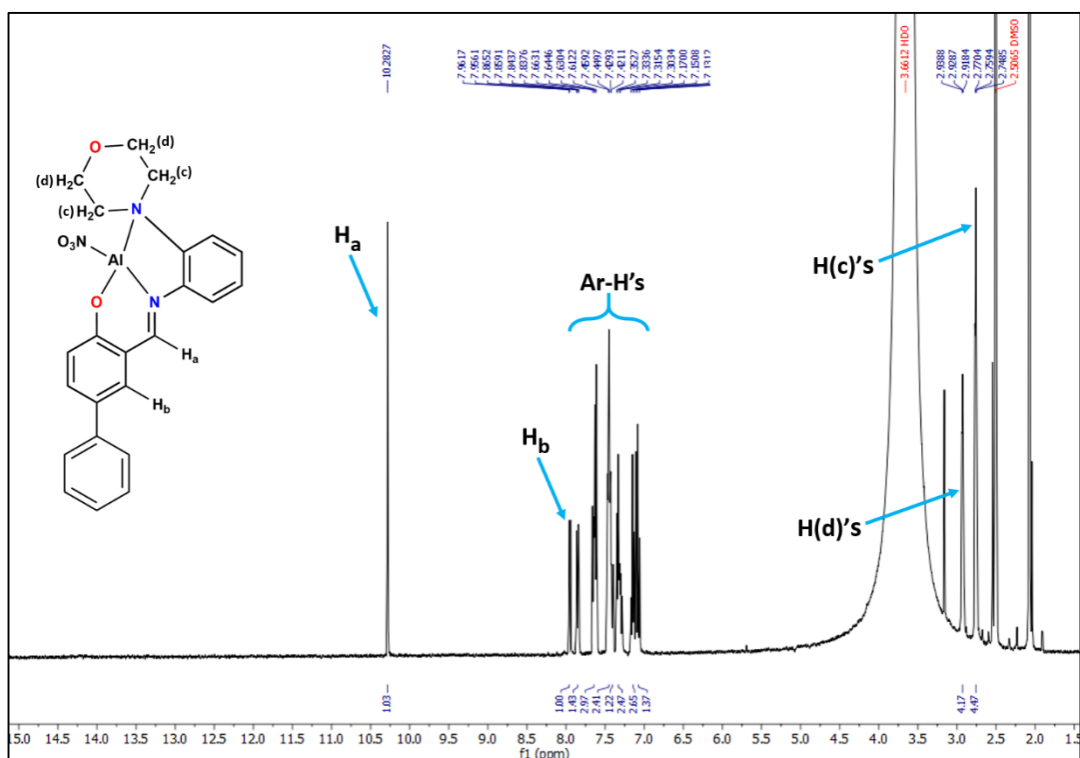


Figure S3: ¹H NMR (300 MHz) spectra of the PIMB-Al³⁺ in DMSO-d₆.

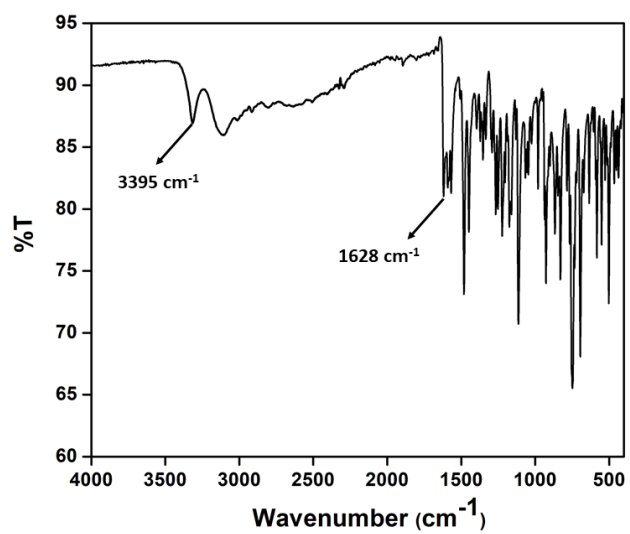


Figure S4: IR spectra of the PIMB.

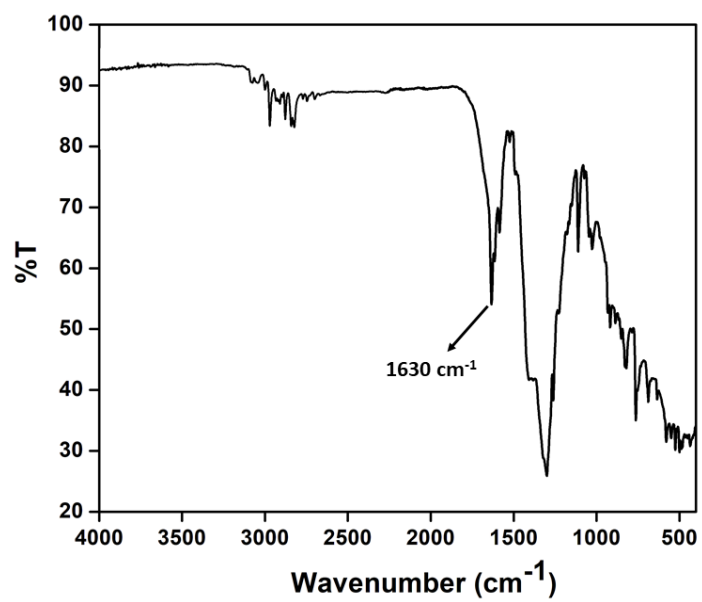


Figure S5: IR spectra of the PIMB-Al³⁺.

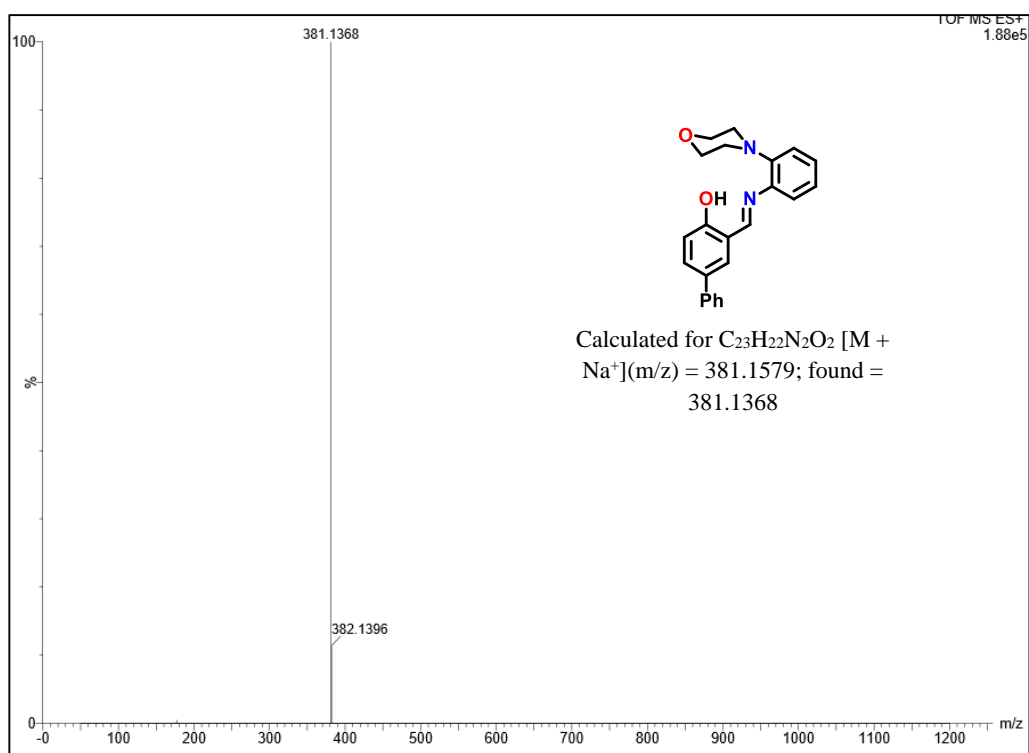


Figure S6: HRMS of the probe (PIMB)

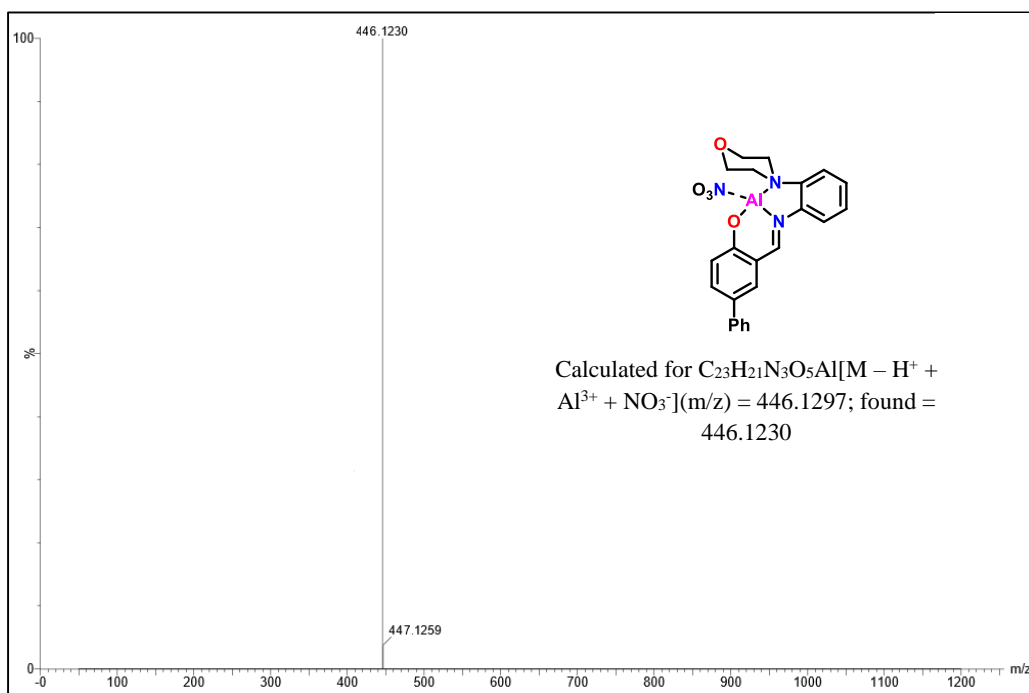


Figure S7: HRMS of the PIMB- Al^{3+}

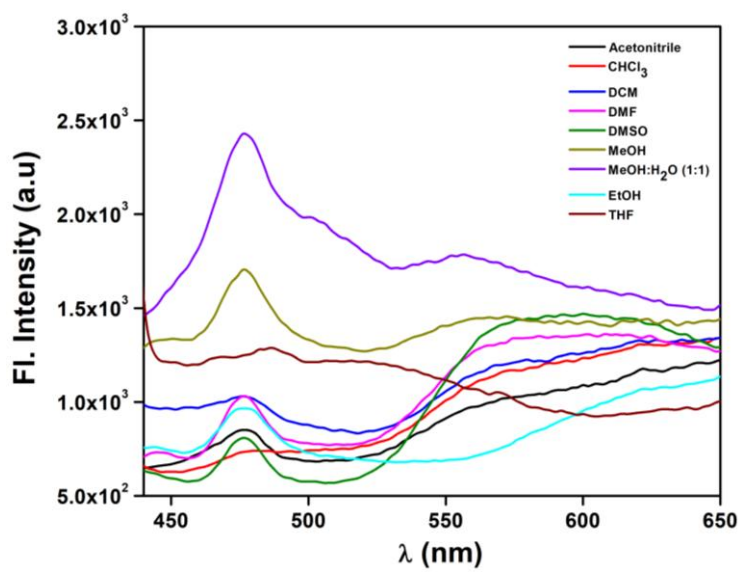


Figure S8: Emission spectra of PIMB in different solvents.

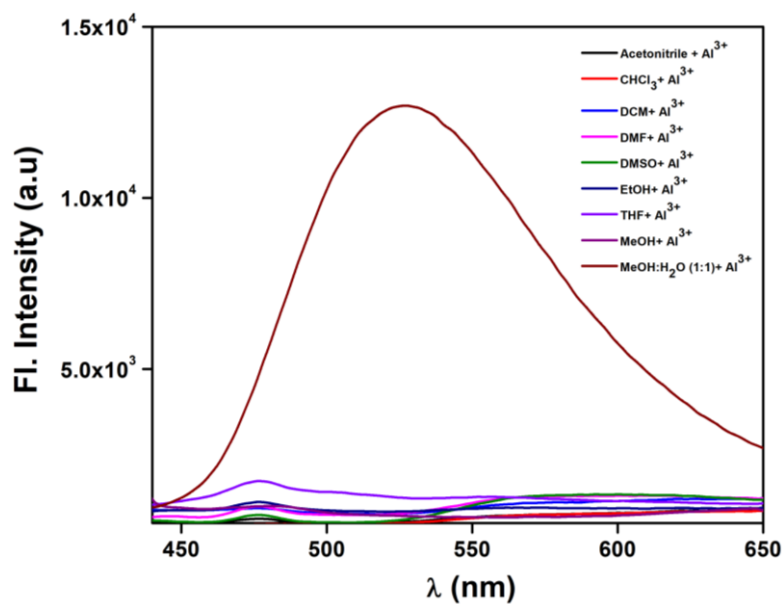


Figure S9: Emission spectra of PIMB- Al^{3+} in different solvents.

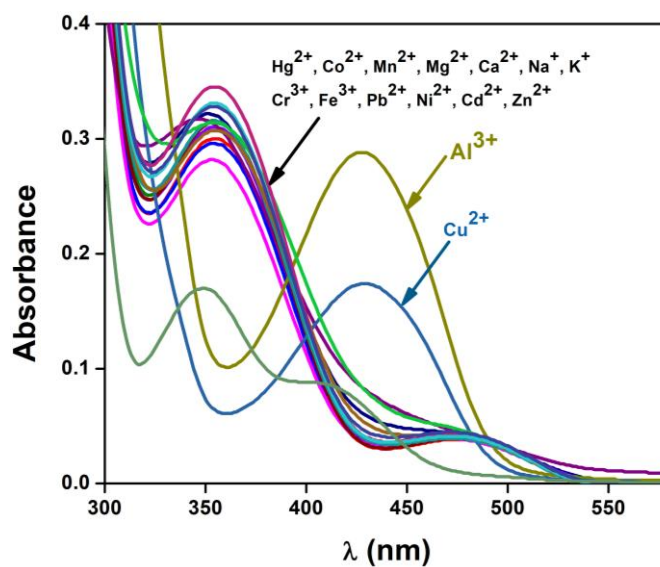


Figure S10: UV-Vis change of PIMB (10 μM) upon addition of different metal ions, i.e., Na^+ , K^+ , Ca^{2+} , Mg^{2+} , Mn^{2+} , Hg^{2+} , Zn^{2+} , Cd^{2+} , Co^{2+} , Ni^{2+} , Cu^{2+} , Pb^{2+} , Fe^{3+} and Cr^{3+} (40 μM) in MeOH/ H_2O (1/1, v/v) using HEPES buffered solution at pH=7.2.

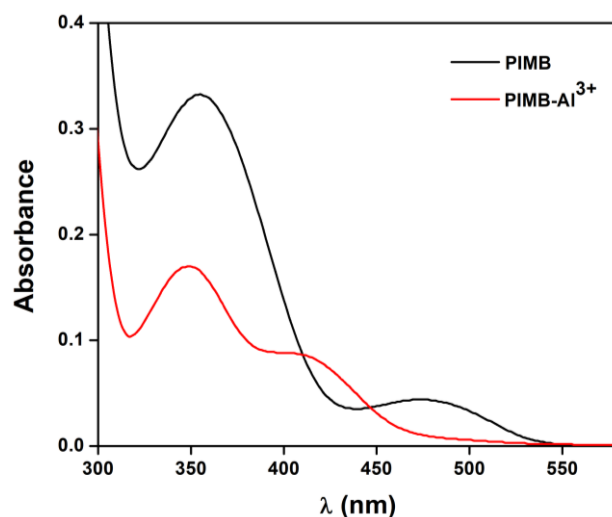


Figure S11: Excitation spectra of PIMB and the PIMB-Al³⁺ complex.

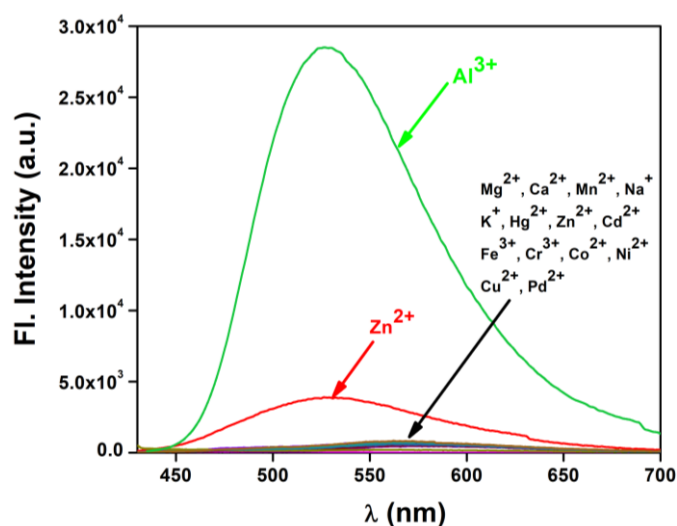


Figure S12: Change in emission intensity of PIMB (10 μM) upon addition of different metal ions, i.e., Mg^{2+} , Ca^{2+} , Mn^{2+} , Na^+ , K^+ , Hg^{2+} , Zn^{2+} , Cd^{2+} , Fe^{3+} , Cr^{3+} , Co^{2+} , Ni^{2+} , Cu^{2+} and Pb^{2+} (40 μM) in $\text{MeOH}/\text{H}_2\text{O}$ (1/1, v/v) using HEPES buffered solution at $\text{pH}=7.2$.

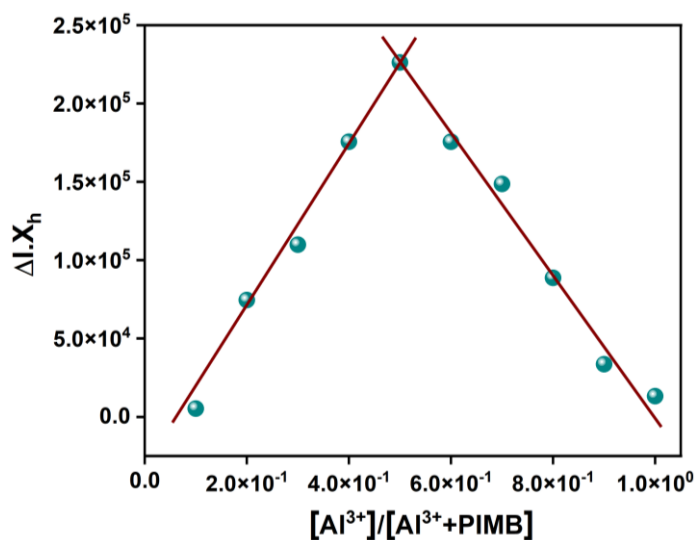


Figure S13: Job's plot of PIMB for Al^{3+} .

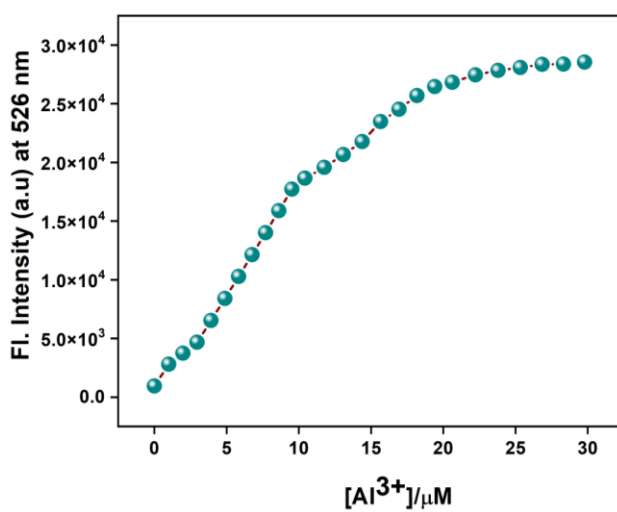


Figure S14: Mole ratio plot of PIMB for Al^{3+} .

Determination of detection limit:

The detection limit was calculated based on the fluorescence titration. To determine the S/N ratio, the emission intensity of PIMB without Al^{3+} was measured by 10 times and the standard deviation of blank measurements was determined. The detection limit of PIMB for Al^{3+} was determined from the following equation¹:

$$DL = K \times S_{b1}/S$$

Where $K = 2$ or 3 (we take 3 in this case); Sb_1 is the standard deviation of the blank solution; S is the slope of the calibration curve.

For Al^{3+} :

From the graph we get slope = 1.94×10^9 and Sb_1 value is 1.97709 .

Thus using the formula, we get the Detection Limit = $(3.06 \pm 0.09) \times 10^{-9}$ M i.e., PIMB can detect Al^{3+} in this minimum concentration through fluorescence techniques.

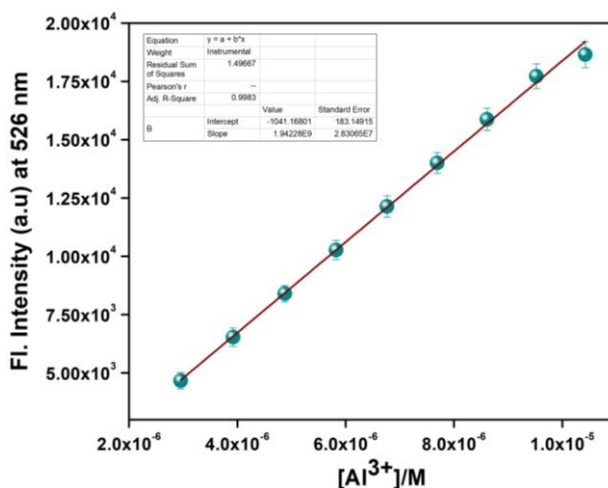


Figure S15: Linear response curve of PIMB at 526 nm depending on the Al^{3+} concentration.

Determination of binding constant from Fluorescence titration data:

Binding constant was calculated according to the Benesi-Hildebrand equation. K_a was calculated following the equation stated below.

$$1/(F-F_0) = 1/\{K_a(F_{max}-F_0) [M^{n+}]^x\} + 1/[F_{max}-F_0]$$

Here F_0 , F and F_{max} indicate the emission in absence of, at intermediate and at infinite concentration of metal ion respectively.

Plot of $1/[F-F_0]$ vs $1/[Al^{3+}]$ gives a straight line indicating 1:1 complexation between PIMB and Al^{3+} where K_a is found to be $2.23 \times 10^5 M^{-1}$ for PIMB.

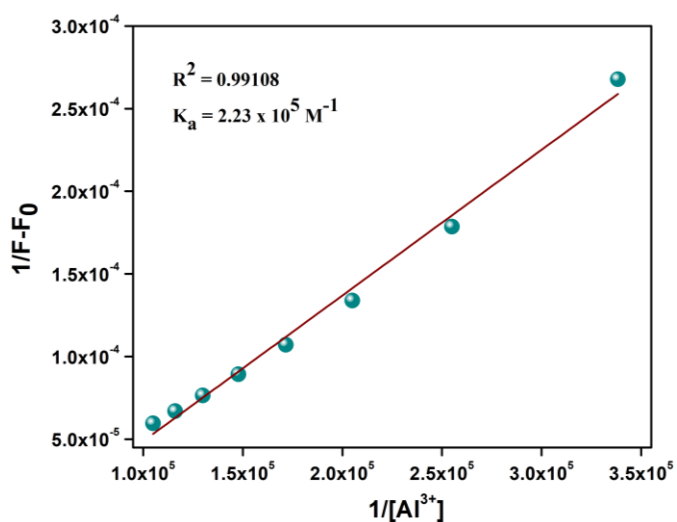


Figure S16: Determination of association constant of PIMB at 526 nm depending on the Al^{3+} concentration using Benesi-Hildebrand equation.

Stability study of PIMB and PIMB- Al^{3+} :

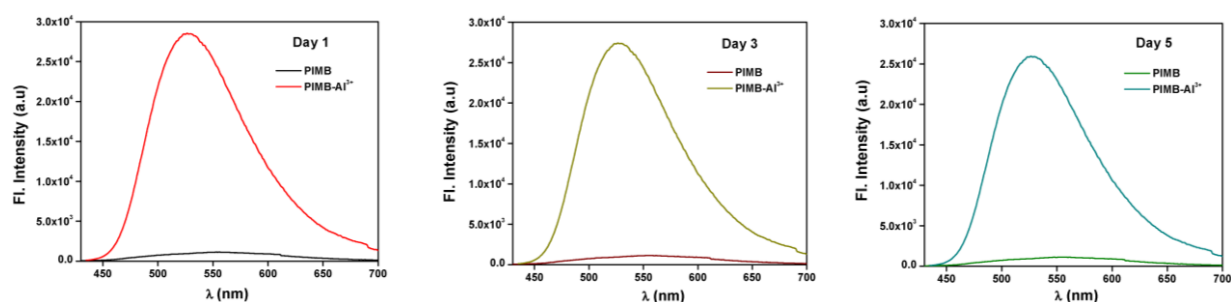


Figure S17: Fluorescence response of PIMB and PIMB- Al^{3+} in MeOH/ H_2O (1/1, v/v) over different days.

pH study:

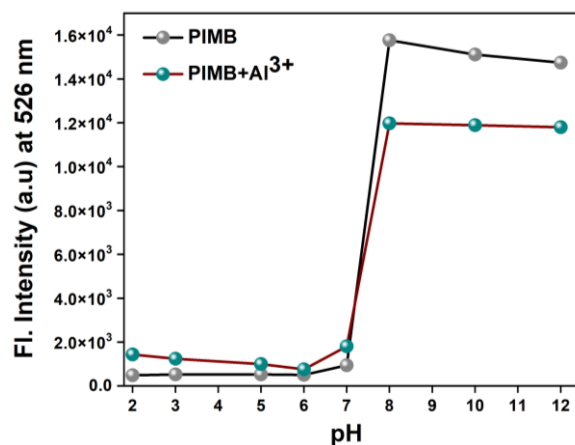


Figure S18: pH study of PIMB for Al^{3+} .

Real water sample analysis:

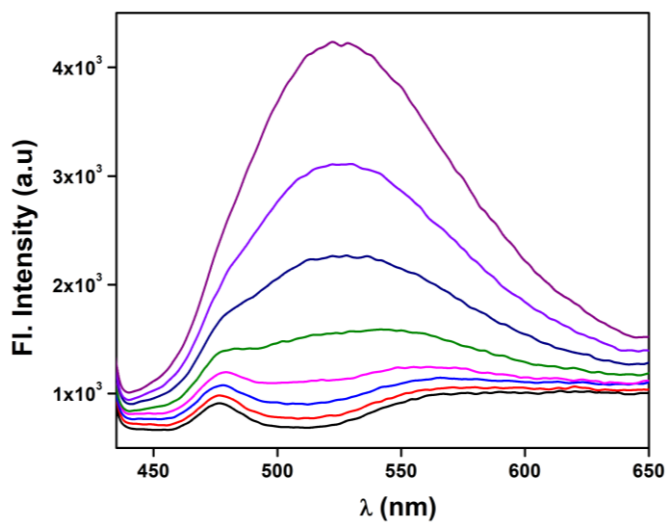


Figure S19: Change in emission spectra of PIMB (15 μM) upon gradual addition of Al³⁺ (0-30μM) in MeOH/H₂O (1/1, v/v) where H₂O part is pond water.

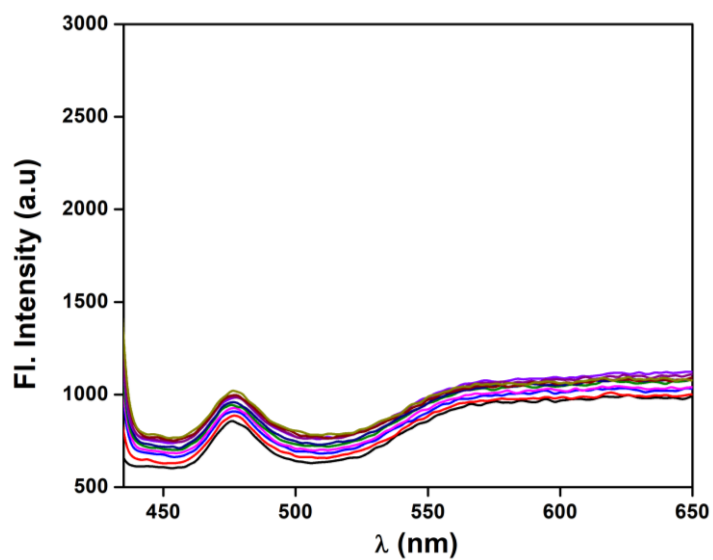


Figure S20: Change in emission spectra of PIMB (15 μM) upon gradual addition of Al³⁺ (0-30μM) in MeOH/H₂O (1/1, v/v) where H₂O part is tap water.

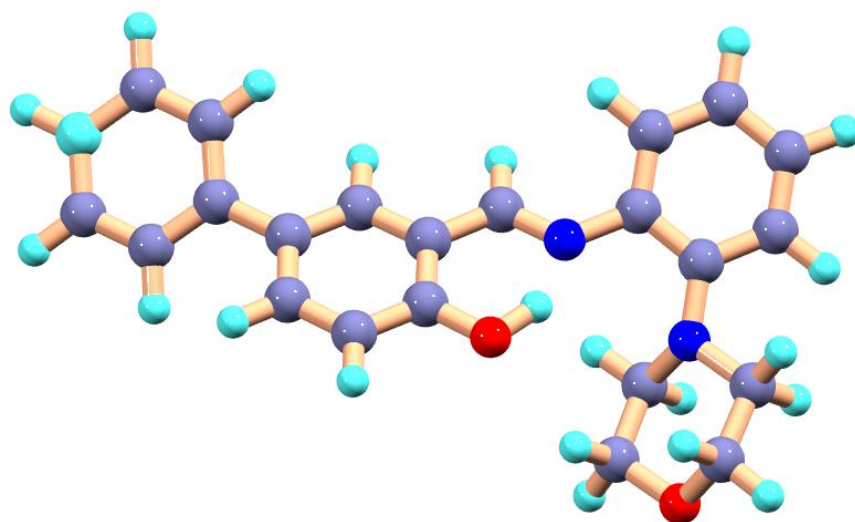


Figure S21. Optimized structure of PIMB calculated by DFT/B3LYP/6-31+G(d) method.

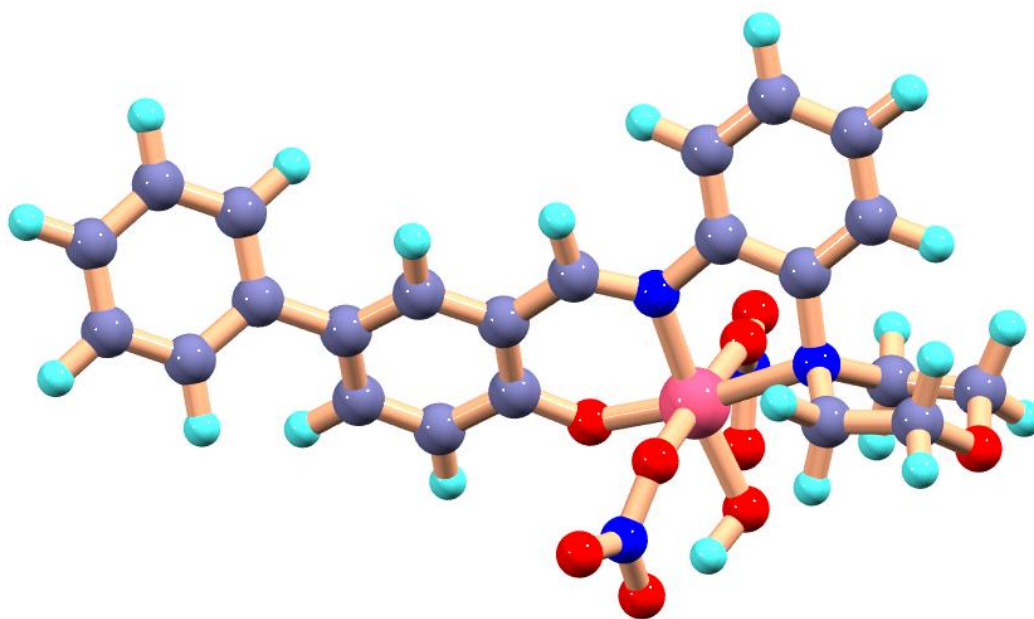


Figure S22. Optimized structure of PIMB-Al³⁺ calculated by DFT/B3LYP/6-31+G(d) method.

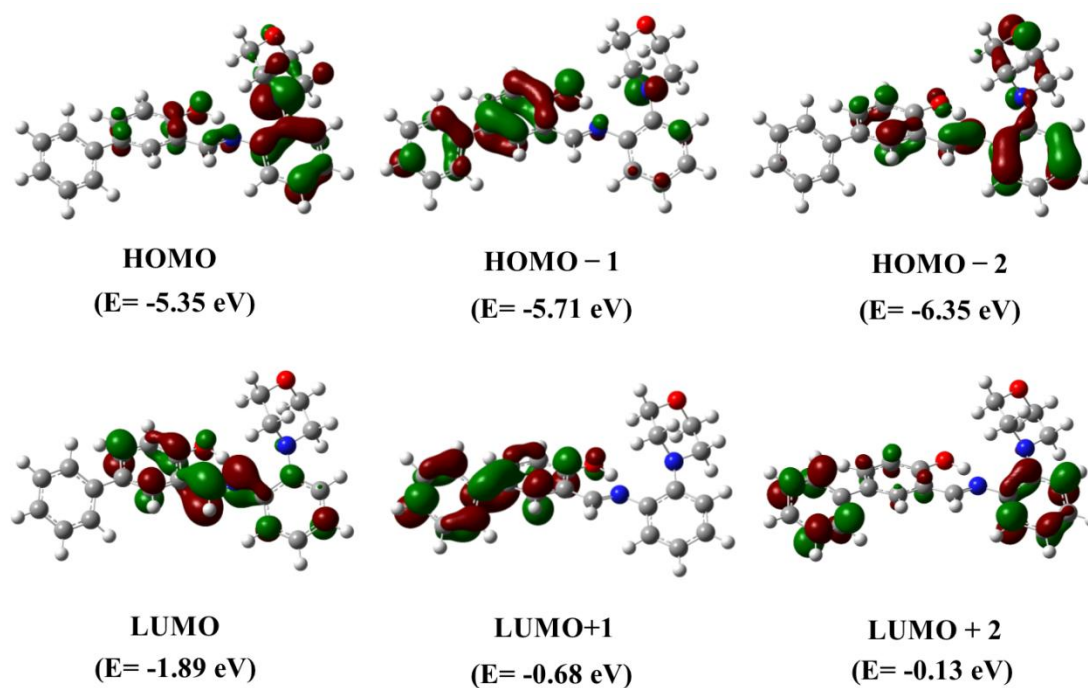


Figure S23.Contour plots of some selected molecular orbitals of PIMB.

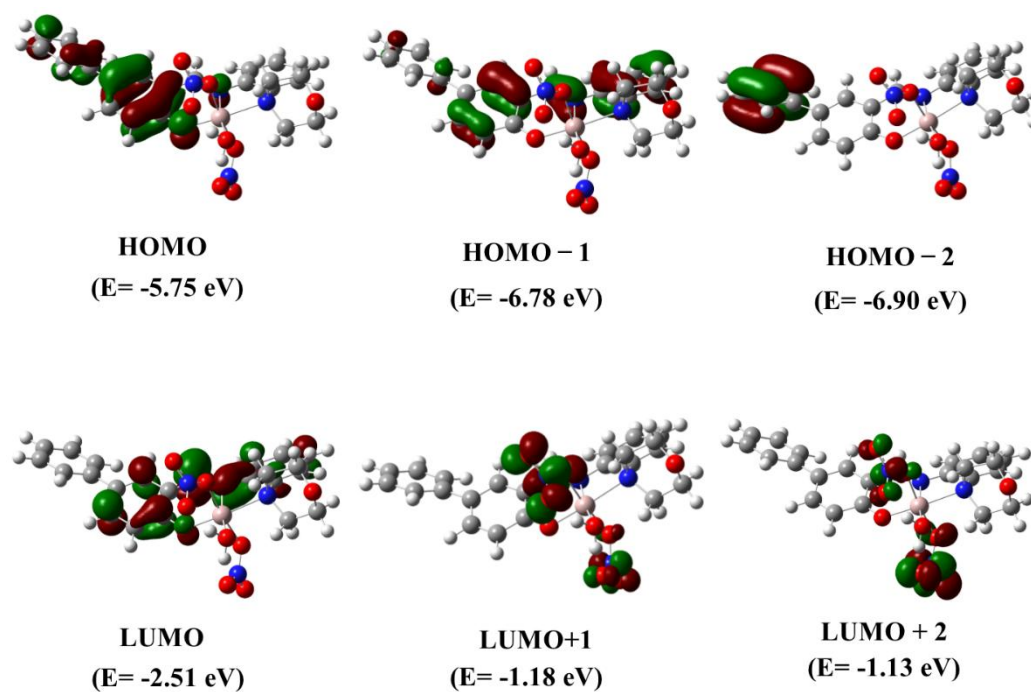


Figure S24.Contour plots of some selected molecular orbitals of PIMB-Al³⁺.

Determination of fluorescence Quantum Yields (Φ) of PIMB and its complex with Al^{3+}

For measurement of the quantum yields of PIMB and PIMB- Al^{3+} , the absorbance of the compounds was recorded in methanol solution. The luminescence quantum yield was then determined using coumarin 153 ($\phi_s = 0.544$) as reference dye. The compounds and the reference dye were excited at the same wavelength and the emission spectra were recorded. The area of the emission spectrum was integrated and the quantum yield is calculated according to the following equation:

$$\phi_S/\phi_R = [A_S / A_R] \times [(Abs)_R / (Abs)_S] \times [n_S^2/n_R^2]$$

Here, ϕ_S and ϕ_R are the luminescence quantum yields of the sample and reference, respectively. A_S and A_R are the area under the emission spectra of the sample and the reference respectively, $(Abs)_S$ and $(Abs)_R$ are the respective optical densities of the sample and the reference solution at the wavelength of excitation, and n_S and n_R are the values of refractive index for the respective solvent used for the sample and reference.

The quantum yields of PIMB and PIMB- Al^{3+} are determined using the above mentioned equation and the values are found to be 0.01 and 0.38 respectively.

Table S1: Table of mole fractions for Job's plot of PIMB and Al^{3+}

V_{PIMB}	$V_{\text{Al}^{3+}}$	$X_{\text{Al}^{3+}}$
0	2.0	1
0.2	1.8	0.9
0.4	1.6	0.8
0.6	1.4	0.7
0.66	1.34	0.67
0.8	1.2	0.6
1	1	0.5
1.2	0.8	0.4
1.34	0.66	0.33
1.4	0.6	0.3
1.6	0.4	0.2
1.8	0.2	0.1
2.0	0	0

Table S2. Energy and compositions of some selected molecular orbitals of PIMB-Al³⁺

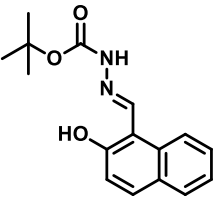
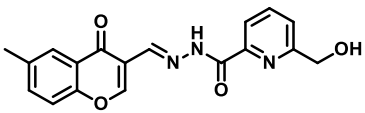
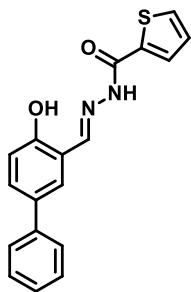
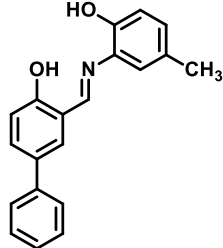
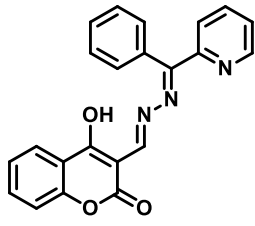
MO	Energy (eV)	% of Composition	
		Al	PIMB
LUMO+5	-0.46	0	100
LUMO+4	-0.69	0	100
LUMO+3	-1.02	0	100
LUMO+2	-1.13	1	99
LUMO+1	-1.18	3	97
LUMO	-2.51	0	100
HOMO	-5.75	0	100
HOMO-1	-6.78	0	100
HOMO-2	-6.90	0	100
HOMO-3	-7.11	0	100
HOMO-4	-7.24	1	99
HOMO-5	-7.45	1	99
HOMO-6	-7.48	1	99
HOMO-7	-7.70	0	100
HOMO-8	-7.89	1	99
HOMO-9	-8.03	1	99
HOMO-10	-8.32	0	100

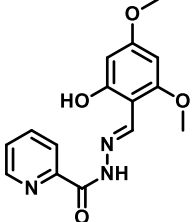
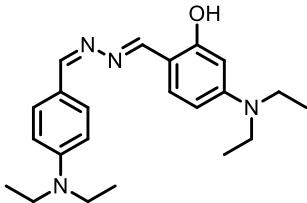
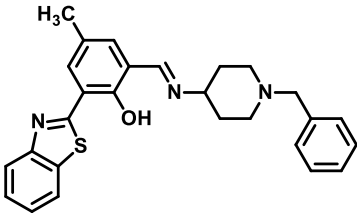
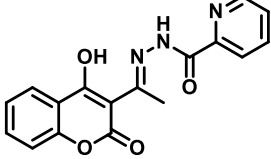
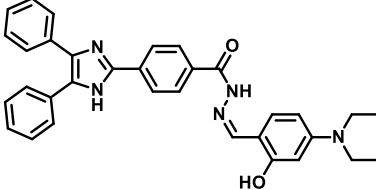
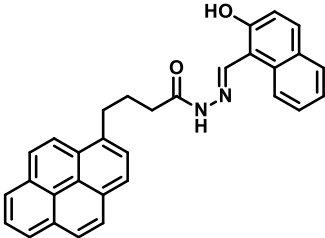
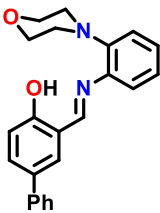
Table S3. Vertical electronic transitions calculated by TDDFT/B3LYP/CPCM method for PIMB and PIMB-Al³⁺ in methanol

Compds.	Energy (eV)	Wavelength (nm)	Osc. strength (f)	Transition	Character
PIMB	2.8263	438.7	0.2573	(98%) HOMO→LUMO	$\pi(L) \rightarrow \pi^*(L)$
	3.3357	371.7	0.0963	(96%) HOMO-1→LUMO	$\pi(L) \rightarrow \pi^*(L)$
	3.8190	324.6	0.2293	(80%) HOMO-2→LUMO	$\pi(L) \rightarrow \pi^*(L)$
	4.1575	298.2	0.0557	(92%) HOMO→LUMO+1	$\pi(L) \rightarrow \pi^*(L)$
	2.9104	426.0	0.2102	(99%) HOMO→LUMO	$\pi(L) \rightarrow \pi^*(L)$

	3.7668	329.1	0.6744	(98%) HOMO-1→LUMO	$\pi(L) \rightarrow \pi^*(L)$
PIMB-	3.6247	342.0	0.0079	(62%) HOMO→LUMO+2	$\pi(L) \rightarrow \pi^*(L)$
Al ³⁺	3.5599	348.3	0.0035	(62%) HOMO→LUMO+1	$\pi(L) \rightarrow \pi^*(L)$

Table S4: The comparison of the present probe (PIMB) with some previous probes for Al³⁺

Probe	Type of response	Lifetime after complexation with Al ³⁺ (ns)	Solvent System	Detection limit	Reference
	Fluorescent turn-on	-	MeOH	3.6×10^{-7} M	[1]
	Fluorescence turn-on	4.24	MeOH/H ₂ O (9:1)	3.12×10^{-7} M	[2]
	Fluorescence turn-on	5.14	CH ₃ CN/H ₂ O, 4/1	$(8.74 \pm 0.36) \times 10^{-9}$ M	[3]
	Fluorescence turn-on	5.02	MeOH/H ₂ O, 4/1	2.24×10^{-7} M	[4]
	Fluorescence turn-on	2.95	MeOH/H ₂ O, 1/1	3.91×10^{-9} M	[5]

	Fluorescence turn-on	0.342	CH ₃ CN/H ₂ O , 1/99	1.32 nM	[6]
	Ratiometric turn-off	-	CH ₃ CN/H ₂ O , 9/1	3.26×10^{-7} M	[7]
	Fluorescence turn-on	4.32	CH ₃ CN/HE PES, 8/2	66 nM	[8]
	Fluorescence turn-on	5.14	MeOH/H ₂ O, 4/1	$(2.64 \pm 0.11) \times 10^{-9}$ M	[9]
	Fluorescence turn-on	-	EtOH/H ₂ O, 1/1	74.75 nM	[10]
	Fluorescence turn-on	4.91	DMSO/H ₂ O, 1/1	2.89×10^{-7} M	[11]
	Fluorescence turn-on	7.67	MeOH/H ₂ O, 1/1	$(3.06 \pm 0.09) \times 10^{-9}$ M	Present Work

References:

1. M. A. Bhat, T. Jan, R. Ashraf, M. Ali, A. Mushtaq, S. A. Bhat, R. J. Butcher and N. U. Din Reshi, *New J. Chem.*, 2026, **50**, 2937.
2. A. Maji, D. Mitra, A. Biswas, M. Ghosh, R. Naskar, S. Gharami N. Murmu and T. K. Mondal, *Sens. Diagn.*, 2024, **3**, 1866.
3. A. Biswas, R. Naskar, D. Mitra, A. Das, S. Gharami, N. Murmu and T. Kumar Mondal, *New J. Chem.*, 2022, **46**, 21968.
4. L. Patra, S. Das, S. Gharami, K. Aich and T. Kumar Mondal, *New J. Chem.*, 2018, **42**, 19076.
5. S. Gharami, K. Aich, P. Ghosh, L. Patra, N. Murmu and T. K. Mondal, *J. Photochem. Photobiol. A. Chem.*, 2020, **390**, 112294.
6. S. R. Jana, K. Saha, A. Chakraborty, A. Das Mahapatra, S. Paul, I. Saha and Chittaranjan Sinha, *Inorg. Chim. Acta*, 2026, **595**, 123098.
7. R. Guleria and S. Swami, *Luminescence*, 2026, **41**, 70432.
8. S. Paul, R. Ghanti, A. Chakrabarty, C. Das, S. Sarkar and S. Goswami, *J. Lumin.*, 2026, **292**, 121749.
9. A. Maji, R. Naskar, D. Mitra, S. Gharami, N. Murmu and T. K. Mondal, *J. Fluoresc.*, 2023, **33**, 2403.
10. J. Wang, L. Ren, Y. Liu, P. Wang, Y. Chen and D. Zhang, *J. Fluoresc.*, 2025, **35**, 13267.
11. K. Bhardwaj, R. Yadav, A. Samanta, R. Jangir, B. RanjanJali, SK A. Kumar and S. K. Sahoo, *Chem. Biodiversity*, 2025, **22**, 202401790.